Aus der
Klinik und Poliklinik für Nuklearmedizin
Klinikum der Ludwig-Maximilians-Universität München

Evaluation of non-invasive PET quantification instead of invasive gold-standard methods in preclinical and clinical applications

Dissertation
zum Erwerb des Doktorgrades der Humanbiologie
an der Medizinischen Fakultät
der Ludwig-Maximilians-Universität München

vorgelegt von
Maria Katrin Kerstens geb. Meindl
aus
Wasserburg am Inn

2024

Mit Genehmigung der Medizinischen Fakultät

der Ludwig-Maximilians-Universität München

Erstes Gutachten:	Prof. Dr. Sibylle Ziegler
Zweites Gutachten:	Prof. Dr. Kirsten Lauber
Drittes Gutachten:	Prof. Dr. Clemens Cyran

Dekan:	Prof. Dr. med. Thomas Gudermann
Tag der mündlichen Prüfung:	13.12.2024

Affidavit

Eidesstattliche Versicherung

Kerstens, Maria

Name, Vorname

Ich erkläre hiermit an Eides statt, dass ich die vorliegende Dissertation mit dem Titel:

Evaluation of non-invasive PET quantification instead of invasive gold-standard methods in preclinical and clinical applications

selbständig verfasst, mich außer der angegebenen keiner weiteren Hilfsmittel bedient und alle Erkenntnisse, die aus dem Schrifttum ganz oder annähernd übernommen sind, als solche kenntlich gemacht und nach ihrer Herkunft unter Bezeichnung der Fundstelle einzeln nachgewiesen habe.

Ich erkläre des Weiteren, dass die hier vorgelegte Dissertation nicht in gleicher oder in ähnlicher Form bei einer anderen Stelle zur Erlangung eines akademischen Grades eingereicht wurde.

Wasserburg, 07.01.2025

Ort, Datum

Maria Kerstens

Unterschrift Doktorandin bzw. Doktorand

Content

Abbreviations

[^{18}F]FDG	[^{18}F]Fluorodeoxyglucose
[^{18}F]FLT	3'-[^{18}F]fluoro-3'-deoxythymidine
[^{18}F]ML-10	2-(5-[^{18}F]fluoropentyl)-2-methyl malonic acid
AD	Alzheimer's disease
AIF	arterial input function
CBS	corticobasal syndrome
CT	computed tomography
DNA	deoxyribonucleic acid
DVr	distribution volume ratio
HE	Hematoxylin-Eosin
IDIF	image derived input function
LOR	line of response
MRT	magnetic resonance tomography
PET	positron emission tomography
PLT	platelet
PSP	progressive supranuclear palsy
RBC	red blood cell
ROI	region of interest
SUV	standard uptake value
SUVr	standard uptake value ratio
V_T	volume of distribution
V_Tr	volume of distribution ratio
VOI	volume of interest
WBC	white blood cell

1. Abstract

Background

Quantification of molecular processes by means of non-invasive positron emission tomography (PET) is a challenging task of nuclear medicine, involving oncological as well as neurological and cardiological questions. In this context, the pharmacokinetic and regional concentration of radiotracers are approximated using various models and methods and characterized in terms of specific parameters and parametric PET images. In order to develop such quantifying approaches, preclinical and clinical studies are necessary in which correlations and validations are performed with mostly invasive gold-standard methods.

Purpose

This thesis aimed at establishing and evaluating two approaches using non-invasive PET instead of invasive gold-standard methods to visualize cellular mechanisms in the context of radiation-induced cellular damage and cerebral processes in neurological issues.

Methods

First approach: Longitudinal PET imaging with the proliferation radiotracer 3'-[^{18}F]fluoro-3'-deoxythymidine ([^{18}F]FLT) and apoptosis radiotracer 2-(5-[^{18}F]fluoropentyl)-2-methyl malonic acid ([^{18}F]ML-10) was performed over a six-month period at defined time points in wild-type mice irradiated with different irradiation doses (0 Gy, 0.5 Gy, 1 Gy, 3 Gy). On the one hand, this was correlated and validated with histological and immunohistochemical examinations with Hematoxylin-Eosin (HE), Ki-67 and cleaved Caspase3 staining. On the other hand with analyses of white blood cells (WBC), red blood cells (RBC) and platelets (PLT). Furthermore, biodistribution studies with the radiotracers [^{18}F]FLT and [^{18}F]ML-10 were performed. *Second approach:* In healthy controls and patients with Alzheimer's disease (AD) and progressive supranuclear palsy (PSP), aggregated tau deposits were visualized by [^{18}F]PI-2620 PET and, in this context, arterial input functions were obtained by continuous sampling of radial artery whole blood. These were validated with non-invasive image-derived input functions (IDIF) generated by manual and automated extraction of the carotid artery in the corresponding PET image. Volumes of distribution (V_T) and volume of distribution ratios (V_Tr) were calculated with the input functions using Logan plots and compared with quantitative parameters such as standard uptake value ratios (SUVr) and distribution volume ratios (DVr) determined by simplified reference tissue modeling.

Results

First approach: The [^{18}F]FLT signal of the hematopoietic bone marrow correlated strongly with blood parameters, especially WBC, and histological as well as immunohistochemical data. Regarding other organs, such as the gastrointestinal tract and thymus, there were some correlations between the data of [^{18}F]FLT PET and invasive gold-standard methods, but also unexpected, non-correlating data that need further investigation, as it does the [^{18}F]ML-10 signal of the hematopoietic bone marrow. The biodistribution data showed strong variations with high standard deviations, which were attributed to difficulties in the technical performance. *Second approach:* AIF highly correlated with IDIF regardless of the manual or automated extraction method. V_T revealed considerable variance across groups, which was strongly reduced by calculating V_Tr. V_Tr and DVr outperformed V_T and SUVr in detecting differences between healthy controls and PSP patients, whereas all quantification parameters performed similarly in comparison of healthy controls and AD patients.

Conclusion

With appropriate radiotracers, non-invasive PET can visualize and quantify biological processes such as proliferation and apoptosis or tau deposition in vivo. In the course of testing and evaluating these quantifications, there are often performed validations with invasive gold-standard methods: Histology is suitable for the validation of PET imaging cellular processes, the measurement of activity concentration in tissue or blood is suitable for the validation of image-based determinations of activity concentration. It is important to be aware of sources of error and limitations, even with gold-standard methods, as the example of biodistribution showed.

2. Zusammenfassung

Hintergrund

Die Quantifizierung molekularer Prozesse mittels der nicht-invasiven Positronen-Emissions-Tomographie (PET) ist ein anspruchsvolles Aufgabengebiet der Nuklearmedizin, das sowohl onkologische, als auch neurologische und kardiologische Fragestellungen betrifft. Dabei werden die Pharmakokinetik und die regionale Konzentration von Radiotracern mittels verschiedener Modelle und Methoden näherungsweise beschrieben und in Form von spezifischen Parametern und parametrischen PET-Bildern charakterisiert. Um solche quantifizierenden Ansätze zu entwickeln, sind präklinische und klinische Studien notwendig, in denen Korrelierungen und Validierungen mit Goldstandard-Methoden, meist invasiver Art, durchgeführt werden.

Zielsetzung

Ziel dieser Arbeit war es, zwei Ansätze zu entwickeln und zu evaluieren, die mittels nicht-invasiver PET anstelle von invasiven Goldstandard-Methoden zelluläre Mechanismen im Kontext von strahleninduzierten Zellschäden und zerebrale Prozesse bei neurologischen Fragestellungen visualisieren.

Methoden

Erster Ansatz: Longitudinale PET-Bildgebung mit dem Proliferations-Radiotracer 3'-[^{18}F]fluoro-3'-deoxythymidine ([^{18}F]FLT) und dem Apoptose-Radiotracer 2-(5-[^{18}F]fluoropentyl)-2-methyl malonic acid ([^{18}F]ML-10) wurde über einen Zeitraum von sechs Monaten zu definierten Zeitpunkten an Wildtyp-Mäusen durchgeführt, die mit unterschiedlichen Bestrahlungsdosen (0 Gy, 0.5 Gy, 1 Gy, 3 Gy) bestrahlt worden sind. Dies wurde einerseits mit histologischen und immunhistochemischen Untersuchungen unter Verwendung von Hematoxylin-Eosin- (HE), Ki-67- und cleaved Caspase3-Färbungen korreliert und validiert. Andererseits mit Analysen der weißen (WBC) und roten (RBC) Blutkörperchen sowie der Blutplättchen (PLT). Außerdem wurden Biodistributionsuntersuchungen mit den Radiotracern [^{18}F]FLT und [^{18}F]ML-10 durchgeführt. *Zweiter Ansatz:* Bei gesunden Kontrollen und Patienten mit Alzheimer-Krankheit (AD) und progressiver supranukleärer Blickparese (PSP) wurden aggregierte Tauablagerungen mittels [^{18}F]PI-2620 PET dargestellt und dabei arterielle Eingangsfunktionen durch die kontinuierliche Entnahme von aus der Radialarterie stammendem Vollblut erhoben. Diese wurden mit Eingangsfunktionen validiert, die durch manuelle und automatisierte Segmentierung der Arteria Carotis im zugehörigen PET-Bild ermittelt wurden. Aus den Eingangsfunktionen wurden mittels Logan-Plots volumes of distribution (V_T) und volume of distribution ratios (V_Tr) berechnet und mit quantitativen Parametern wie standard uptake value ratios (SUVr) und durch simplified reference tissue modeling ermittelte distribution volume ratios (DVr) verglichen.

Ergebnisse

Erster Ansatz: Das [^{18}F]FLT Signal des hämatopoetischen Knochenmarks korrelierte stark mit den Blutparametern, insbesondere den WBC, und den histologischen und immunhistochemischen Daten. Bei anderen Organen, wie dem Gastrointestinaltrakt und Thymus, lagen stellenweise Korrelationen zwischen den Daten des [^{18}F]FLT PET und der invasiven Goldstandard-Methoden vor. Es gab aber auch unerwartete, nicht-korrelierende Daten, die weitere Untersuchungen erfordern, ebenso wie das [^{18}F]ML-10 Signal des hämatopoetischen Knochenmarks. Die Daten der Biodistribution zeigten eine starke Streuung mit hohen Standardabweichungen, die auf Schwierigkeiten in der technischen Durchführung zurückgeführt wurden. *Zweiter Ansatz:* Die arteriellen Eingangsfunktionen korrelierten in hohem Maße mit den aus dem PET-Bild abgeleiteten

Eingangsfunktionen, unabhängig davon, ob die Segmentierung der Arteria Carotis manuell oder automatisiert durchgeführt wurde. V_T wiesen gruppenübergreifend erhebliche Schwankungen auf, die bei der Berechnung von V_Tr stark verringert wurden. V_Tr und DVr zeigten in der Erkennung von Unterschieden zwischen gesunden Kontrollen und PSP Patienten bessere Ergebnisse als V_T und SUVr. Beim Vergleich von gesunden Kontrollen und AD Patienten haben alle Quantifizierungsparameter ähnlich abgeschnitten.

Schlussfolgerung

Die nicht-invasive PET kann mit geeigneten Radiotracern biologische Prozesse, wie die Proliferation und Apoptose oder Tau-Ablagerungen, in vivo darstellen und quantitativ bestimmen. Im Zuge der Erprobung und Evaluierung dieser Quantifizierungen werden häufig Validierungen mit invasiven Goldstandard-Methoden durchgeführt: Zur Validierung von im PET-Verfahren dargestellten zellulären Prozessen eignet sich die Histologie, zur Validierung von bildbasierten Bestimmungen der Aktivitätskonzentration die Messung der Aktivitätskonzentration im Gewebestück oder Blut. Dabei gilt es auch bei den Goldstandard-Methoden auf Fehlerquellen und Limitationen zu achten, wie sich am Beispiel der Biodistribution zeigte.

3. Introduction

3.1 Overview

Positron emission tomography (PET) is an important part of diagnostics and research in nuclear medicine. Due to the development of PET scanners with improved temporal and spatial resolution, higher sensitivity and a larger axial field of view, molecular processes in tissues and organs can be quantified with increasing precision in vivo (1). This is useful for many medical questions, such as the visualization of cellular mechanisms in the context of cellular damage or cerebral processes in neurological issues. To fulfill the requirements of clinical day-to-day PET examinations, sensitive and specific radiotracers are fundamental, as well as a detailed knowledge of their pharmacokinetics, sophisticated imaging protocols and convenient quantification approaches. These components are developed and tested in preclinical and clinical studies and need validation with gold-standard methods (2, 3).

3.2 Objective of this thesis

This thesis aimed at establishing and evaluating two PET-derived, non-invasive approaches to replace invasive gold-standard methods.

The first approach included longitudinal PET imaging in a mouse model of increased proliferative and apoptotic cell processes induced by whole body irradiation. This was validated with several invasive gold-standard methods, some of them requiring euthanasia, namely histological and immunohistochemical examinations, biodistribution, and analysis of blood parameters (Figure 1A).

The second approach was performed in a clinical setting in the context of the detection of the activity concentration in blood over time for absolute [^{18}F]PI-2620 PET quantification used in the diagnosis of neurodegenerative diseases. Here, non-invasive image derived input functions (IDIF) were obtained as an alternative to arterial input functions (AIF), which represent the gold-standard but involve an uncomfortable, invasive procedure associated with high personnel effort and burden to the patients. Two different methods were used to determine the IDIF, one that involved manual segmentation and one that involved automated segmentation (Figure 1B). With both the IDIF and AIF, several quantification parameters were calculated and compared.

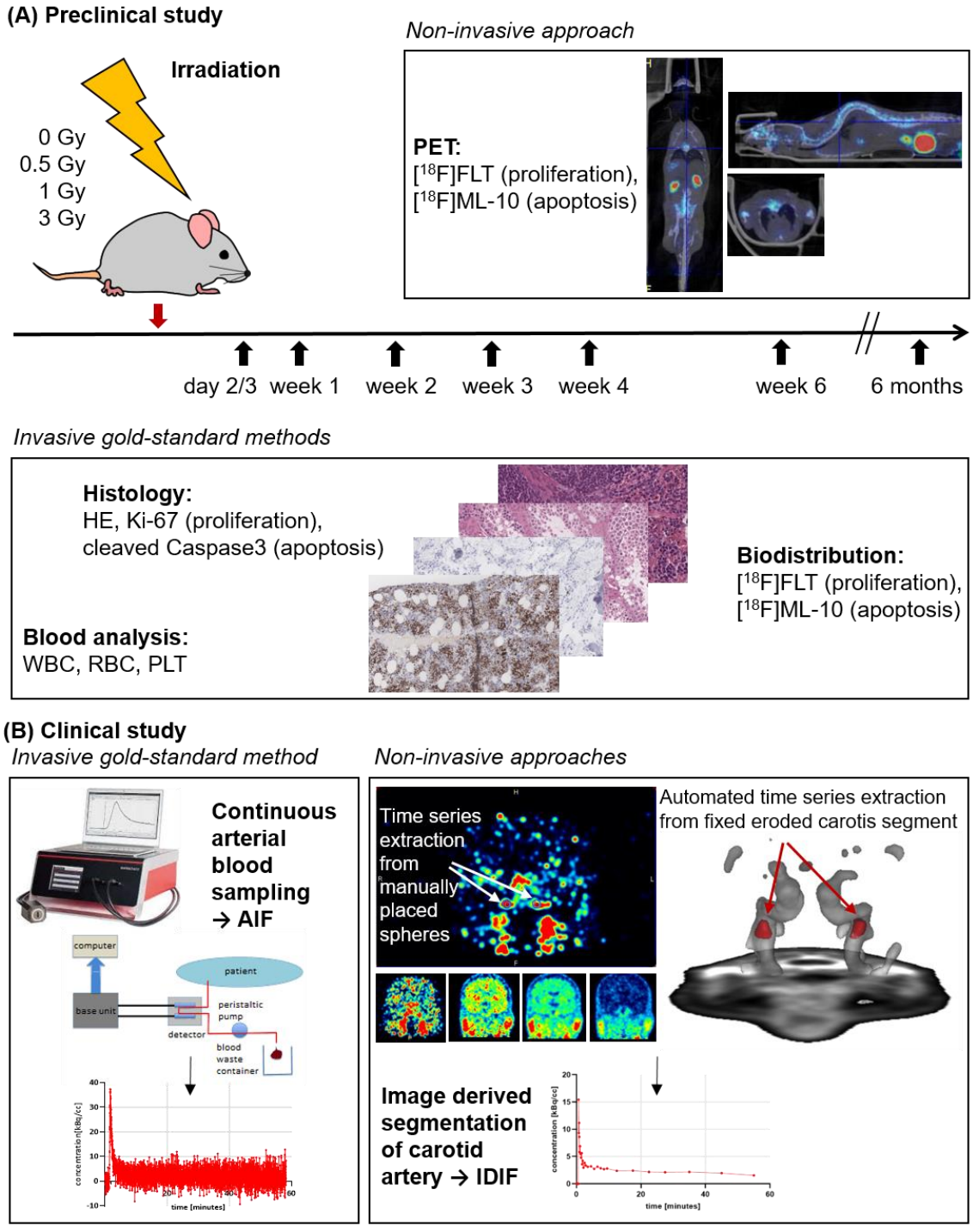

Figure 1: Thesis objective. Establishment and evaluation of non-invasive, PET derived approaches to replace invasive gold-standard methods. (A) Preclinical study: Longitudinal PET imaging with proliferation and apoptosis radiotracers in a mouse model after whole-body irradiation with different irradiation doses. Validation with euthanasia-requiring, invasive gold-standard methods: histological and immunohistochemical examinations with Hematoxylin-Eosin (HE), Ki-67 and cleaved Caspase3 staining; analysis of white blood cells (WBC), red blood cells (RBC) and platelets (PLT); biodistribution with a proliferation and apoptosis radiotracer. (B) Clinical study: Acquisition of IDIF by manual und automated segmentation of the carotid artery as an alternative to gold-standard AIF obtained by continuous arterial blood sampling. Calculation and comparison of several [18F]PI-2620 quantification parameters using AIF and IDIF.

3.3 Positron emission tomography (PET)

PET is a nuclear medicine in vivo imaging technique for visualization and measurement of molecular processes in tissues and organs of humans and animals. The physical principle underlying PET is annihilation coincidence detection. Therefore, it is necessary to inject (usually intravenously) a radiotracer into the bloodstream of the subject. This is a carrier substance labeled with a radioisotope (e.g. ^{18}F, ^{68}Ga, ^{124}I, ^{64}Cu), which takes part in a biological process in the tissue of interest. To gain stability, the radioisotope decays, converting a proton from the nucleus into a neutron and forming a positron and neutrino:(4, 5)

$$ {}^{1}_{1}p^{+} \rightarrow {}^{1}_{0}n + {}^{0}_{1}\beta^{+} + v $$

As the emitted positron makes its way through the surrounding material associated with directional changes and kinetic energy losses, it collides with an electron, which leads to annihilation of both particles. Thereby two photons are emitted simultaneously at almost exactly 180° to each other, both with an energy of 511 keV (Figure 2 A). The photons are detected by so-called electronic collimation, which involves the detection of coincidence events with two opposing detectors contained in a ring of scintillation crystals (Figure 2 B). Through the process of scintillation, the energy of the detected photons is converted into light, which is then quantified using a photomultiplier. The detection follows a temporal acceptance criterion, which means that only photons detected in a certain time window are assumed to originate from the same annihilation and are thus detected as coincidence event. With the line of response (LOR), which connects the centers of the detector pair used for the detection of the two photons, it is possible to narrow down the localization of the positron-electron annihilation and photon emission (Figure 2 B).(5, 6)

A **B**

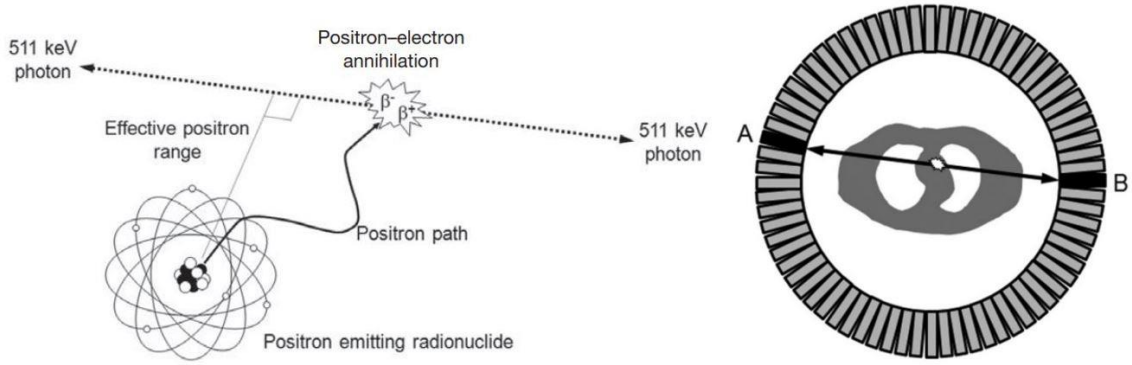

Figure 2: Principles of annihilation coincidence detection (6). (A) β⁺-decay with positron-electron-annihilation and creation of two 511 keV photons. (B) Detection of a co-incidence event with a detector ring consisting of scintillation crystals.

Depending on the imaging protocol, the PET scan starts during the radiotracer injection or a certain time after radiotracer injection. In both cases, the coincidence events and their related time points are recorded according to the mentioned functionalities and criteria, which are the basis for the reconstruction of a tomographic, three-dimensional PET image using mathematical algorithms such as backprojection techniques or iterative methods. Thereby static or dynamic PET images can be generated depending on whether the coincidence events are integrated over the entire acquisition time interval or over several split time frames. In order to avoid image artefacts and to achieve the best possible agreement between the intensity of the PET image and the actual activity concentrations, some corrections are performed, such as corrections for random

coincidences, scattered radiation, attenuation and dead time. By calibrating the PET scanner with a phantom, the activity concentration ([Bq/ml]) can be specified for each voxel. Meanwhile, most PET scanners are hybrid devices, meaning that they also contain computed tomography (CT) or magnetic resonance tomography (MRT). This makes it possible to generate fusion images that facilitate anatomical or structural assignment.(4, 5)

3.3.1 Radiotracer

In the following, the mechanisms, properties and current clinical applications of the radiotracers used in the investigations of this thesis are characterized. All of them incorporate the radionuclide ^{18}F with a half-life of 109.8 minutes.

3.3.1.1 3'-[^{18}F]fluoro-3'-deoxythymidine ([^{18}F]FLT)

Proliferation is a physiological metabolic process in which cells multiply through cell division and cell growth. Increased proliferation occurs after cell damage or in cancer. The radiotracer 3'-[^{18}F]fluoro-3'-deoxythymidine ([^{18}F]FLT) is used for PET imaging of proliferation.(7)

The binding mechanism of [^{18}F]FLT is based on the thymidine salvage pathway and deoxyribonucleic acid (DNA) thymidine synthesis pathway. In simple terms, proliferating cells thereby receive increased amounts of the circulating molecule thymidine and closely related analogs, which are phosphorylated and then support DNA synthesis. [^{18}F]FLT is very similar to thymidine and binds to the DNA of proliferating cells.(8)

[^{18}F]FLT has been mostly used in preclinical and clinical observational studies concerning tumor patients. These showed that [^{18}F]FLT was suitable for detection, diagnosis and staging of several tumor types (8). [^{18}F]FLT PET has also been found to be useful in early predicting treatment response to therapeutic interventions such as chemotherapy, radiotherapy and chemoradiotherapy (9, 10). This involved obtaining information on tumor biology, more specifically tumor proliferation heterogeneity before, during, and after treatment, which was not possible by biopsy samples (9). In some studies, [^{18}F]FLT has been shown to have higher tumor specificity and fewer false-positive signals due to infection or inflammation compared with [^{18}F]Fluorodeoxyglucose ([^{18}F]FDG), which is the standard radiopharmaceutical used for tumor diagnosis (11-13). A few studies have been performed using [^{18}F]FLT PET to investigate the detection of radiation-induced tissue injury, particularly of the bone marrow (14-18). They showed statistically significant correlations between the irradiation dose and [^{18}F]FLT uptake.

3.3.1.2 2-(5-[^{18}F]fluoropentyl)-2-methyl malonic acid ([^{18}F]ML-10)

Apoptosis is a form of cellular suicide program that, unlike other cell death mechanisms such as necrosis, does not involve inflammatory processes. It occurs in the context of cell homeostasis as well as in a number of diseases. Apoptosis can be activated by external cellular stimuli (extrinsic pathway) or by internal cellular stress signals (intrinsic pathway). The radiotracer 2-(5-[18F]fluoropentyl)-2-methyl malonic acid ([18F]ML-10) is used for PET imaging of apoptosis.(7, 19)

The binding mechanism of [^{18}F]ML-10 is based on processes that occur in early stages of apoptosis, namely changes in plasma membrane potential, phospholipid scramblase activity, and cellular acidification (20). [^{18}F]ML-10 recognizes cells undergoing such processes, crosses their plasma membranes and accumulates in their cytoplasm (21).

[^{18}F]ML-10 has been used in many preclinical but also clinical studies. A frequently investigated topic was its suitability for measuring apoptosis as an indicator of cancer treatment response with the aim of avoiding ineffective treatment in non-responders (22-27). Depending on tumor type and treatment method, conflicting results were obtained (22). There have also been studies investigating whether [^{18}F]ML-10 PET can be used to visualize apoptotic processes due to myocardial infarction (28, 29), cerebral stroke (21) or atherosclerosis (30). Studies evaluating [^{18}F]ML-10 PET for the investigation of radiation-induced tissue injury have not been published so far.

3.3.1.3 [^{18}F]PI-2620

The pathology of tauopathies, a group of neurodegenerative diseases such as Alzheimer's disease (AD), progressive supranuclear palsy (PSP) or corticobasal syndrome (CBS), is characterized by the aggregation of hyperphosphorylated microtubule-associated tau protein in neurons and glia of the brain. [^{18}F]PI-2620 is a so-called second generation tau-PET radiotracer used for diagnosis of such diseases.(31)

The binding mechanism of [^{18}F]PI-2620 depends on the structural, energetic, and kinetic properties of the tau proteins accumulating in the respective tauopathie (32). According to these, [^{18}F]PI-2620 binds to the surface sites, core sites or entry sites of the tau proteins (33).

Many clinical studies have been performed to investigate and evaluate the diagnostic value of [^{18}F]PI-2620 PET. In contrast to some first generation tau-PET radiotracers, [^{18}F]PI-2620 showed less off-target binding and good properties to detect not only tau accumulation in AD but also in non-AD tauopathies (34-41). Due to this, [^{18}F]PI-2620 is meanwhile used in tertiary centers.

3.3.2 Quantification of radiotracer pharmacokinetics

In the following, the essential quantification parameters and methods used in the investigations of this thesis are described.

3.3.2.1 Standard uptake value (SUV)

Besides the visual interpretation of PET images, the determination of standard uptake values (SUV) is a simple and widely used quantification method in preclinical and clinical routine:

$$SUV\ [-] = \frac{activity\ concentration\ \left[\frac{Bq}{g}\right]}{injected\ activity\ [Bq] \times subject\ weight\ [g]}$$

The activity concentration derives from the PET signal. For this, regions of interest (ROI) or volumes of interest (VOI) are placed in specific organs or tissues displayed on the PET image. Based on their mean or maximum voxel value, the activity concentration is obtained. Whereas the SUV calculated with the mean voxel value may be biased by distorted voxel values at the boundary of the ROI or VOI due to limited resolution, the SUV calculated with the maximum voxel value may be inaccurate because it is based on only one voxel. Concerning this, there is an approach to calculate the maximum voxel value based on the five hottest voxels of the ROI or VOI.(42, 43)

By calculating dimensionless SUV and thus avoiding variability due to subject-specific weight and injected radiotracer dose, inter- and intrapatient comparisons can be performed. To further reduce variability, it may be useful to perform a normalization with the SUV of a reference tissue in which no specific radiotracer accumulations are expected. The resulting parameter is called standard uptake value ratio (SUVr).

3.3.2.2 Volume of distribution (V_T)

The pharmacokinetic of a radiotracer describes its temporal and spatial distribution within the body. It depends on the interaction of a number of components such as the radiotracer dose, absorption, blood flow, tissue binding, metabolisation and elimination.(4)

To characterize these physiological and biochemical processes in an approximate way, compartment models can be used. Here, the body is divided into one or more compartments, which represent a fictive volume (e.g. organs, organ clusters, parts of organs, tissue types) wherein the injected radiotracer is homogenously distributed, with gradients in time but not in space. Rate constants are used to describe mass transport into, out of and between the different compartments.(44)

In the one-compartment model, the entire body or a certain tissue is seen as a single central compartment, named the tissue compartment, in which the radiotracer is distributed with the time-dependent concentration $C_T(t)$. This interacts with the blood compartment, into which the radiotracer is delivered after its injection. The time-dependent radiotracer concentration in the arterial plasma of the blood compartment is named $C_P(t)$. By the rate constants k1 and k2, the reversible, bidirectional mass transport between the two compartments is described:(4)

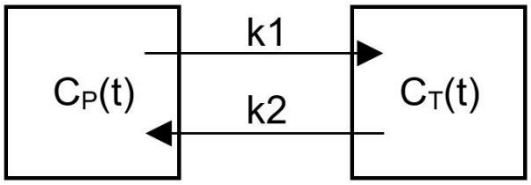

Figure 3: One-compartment model. Reversible, bidirectional mass transport between the blood and tissue compartment with the time-dependent concentrations $C_P(t)$ and $C_T(t)$ described by the rate constants k1 and k2.

The mass balance between the blood compartment and the tissue compartment can be expressed with a first-order ordinary differential equation by subtracting the flux out of the tissue compartment from the flux into the tissue compartment:

$$\frac{dC_T(t)}{dt} = k_1 C_P(t) - k_2 C_T(t)$$

Based on this kinetic model and its differential equation, the volume of distribution (V_T) is an important parameter in pharmacokinetics. It relates the amount of radiotracer in the entire body to the concentration of the radiotracer in arterial plasma and describes the volume of arterial plasma that would be required to absorb the same amount of radiotracer as contained in the entire body. In the one-compartment model, V_T can be determined at equilibrium by the quotient of $C_T(t)$ and $C_P(t)$, which equals the quotient of the rate constants:(45)

$$\frac{dC_T(t)}{dt} = 0 \quad \rightarrow \quad V_T = \frac{C_T(t)}{C_P(t)} = \frac{k1}{k2}$$

3.3.2.3 Input function

In order to determine $C_P(t)$, an accurate knowledge of the unmetabolised radiotracer concentration in arterial plasma over time (so-called input function) is necessary.

AIF represent the gold-standard using continuous sampling of blood from the radial artery with an external detector. This is a complex procedure that involves inconvenience and risks to the patient

as well as a high personnel effort (1). Although considered to be the gold-standard, the measurement can be prone to errors, such as clotting on the tube walls. For the best possible estimation of the original time-activity-curve, the whole-blood-to-plasma ratio should be determined and radiometabolite analyses should be performed. Furthermore, corrections for dispersion and delay are necessary (46). Especially the correction for dispersion is not trivial, as it requires kinetic modeling (47).

A non-invasive alternative to the described invasive approach are IDIF. They are obtained directly from the dynamic PET image, preferably from the PET signal of large vascular structures such as the heart, aortic segments or femoral arteries. In brain PET scans, these areas are usually not in the field of view, so blood vessels must be used, the most popular being the carotid artery. PET signals from these regions can be extracted by various approaches, such as manual placement of a VOI, automated voxel intensity based segmentation, use of an atlas, or matching with an associated CT or MRT image. Since the diameter of blood vessels is often smaller than the spatial resolution of PET scanners, artefacts may occur due to partial volume effects, which in turn may distort the obtained IDIF. Due to this, corrections of the partial volume effects may be necessary, which depend on many parameters and are error-prone. There are approaches to calibrate the IDIF with blood samples instead. Discrete blood samples should be collected anyway, as blood to plasma ratio determinations and radiometabolite analyses should also be performed for IDIF.(48-50)

One approach to reduce, but not completely eliminate, arterial blood sampling is so-called minimal invasive blood sampling. This involves the acquisition of an IDIF in combination with the collection of discrete blood samples at defined time points. A commonly used concept is to collect an arterial blood sample at an early and late time point after injection, supplemented with the collection of a few venous blood samples in between. Based on these time-activity values, the IDIF is scaled. In some cases, they are used for the fitting of a population-based input function. As for AIF, radiometabolite analyses, blood-to-plasma ratio determinations, and delay corrections should be performed. Although this approach can circumvent the complex and with several disadvantages associated continuous arterial blood sampling, it cannot achieve the same accuracy.(1, 48, 51)

3.3.2.4 Logan plot

The Logan plot is a graphical analysis method using simplified regression analysis to estimate V_T. By rearranging and integrating the differential equation describing the one-compartment model introduced in chapter 3.3.2.2, and assuming equilibrium in the two compartments after a certain time t*, Logan et al. proposed the following expression:(52)

$$\frac{\int_0^t C_T(\tau)d\tau}{C_T(t)} = V_T \frac{\int_0^t C_P(\tau)d\tau}{C_T(t)} + b$$

The linear fitting of the two fraction terms of the equation results in a linear regression line whose slope, starting from the equilibrium time t*, corresponds to V_T. $C_P(t)$ is determined by one of the methods for obtaining input functions described in chapter 3.3.2.3, whereas $C_T(t)$ is given by the time-activity-curve of a tissue VOI placed in the PET image. Here it should be considered that tissue VOI are sensitive to noise, which can result in an underestimation of V_T.(53, 54)

To reduce variability, it is common to calculate volume of distribution ratios (V_Tr). This is done by dividing the V_T of a specific region by the V_T of a reference region in which no specific radiotracer accumulations and no influence of disease or treatment are expected.

3.3.2.5 Simplified reference tissue model

The simplified reference tissue model is based on the assumptions of the one-compartment model and describes the reversible, bidirectional mass transport between the blood compartment and the tissue compartment without measuring an AIF. Instead, the input function is derived from a reference tissue in which no or only little specific radiotracer binding and a similar nonspecific radiotracer binding as in the tissue of interest is expected. In the plasma of the blood compartment, the radiotracer is distributed with the time-dependent concentration $C_P(t)$, in the tissue compartment with $C_T(t)$ and in the reference tissue compartment with $C_T(t)'$. The mass transport between the blood compartment and the tissue compartment is described with the rate constants k1 and k2, that between the blood compartment and the reference tissue compartment with the rate constants k1' and k2':(55)

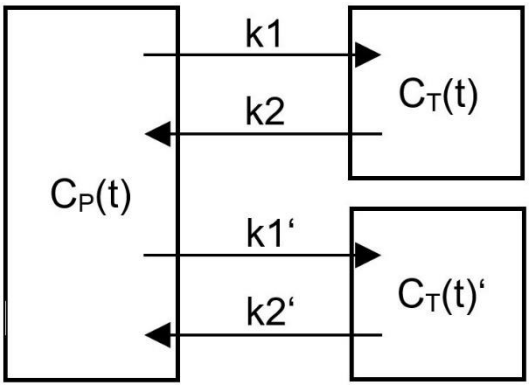

Figure 4: Simplified reference tissue model. Reversible, bidirectional mass transport between the blood, tissue and reference tissue compartment with the time-dependent concentrations $C_P(t)$, $C_T(t)$ and $C_T(t)'$ described by the rate constants k1, k2, k1' and k2'.

The mass balance between the blood compartment and the tissue and reference tissue compartment can be expressed with first-order ordinary differential equations:

$$\frac{dC_T(t)}{dt} = k_1 C_P(t) - k_2 C_T(t)$$

$$\frac{dC_T(t)'}{dt} = k_1' C_P(t) - k_2' C_T(t)$$

As it is assumed that the distribution volume of the non-specifically bound radiotracer in the tissue of interest and in the reference tissue is the same, the time-dependent concentration of the tissue compartment can be expressed as follows (56):

$$\frac{k1}{k1'} = \frac{k2}{k2'} \quad \rightarrow \quad C_T(t) = \frac{k1}{k1'} C_T(t)' + \frac{k1}{k1'}(k_2' - k_2) C_T(t)' \otimes e^{-k_2 t}$$

The distribution volume ratio (DVr) is an important parameter in the simplified reference tissue model and describes the ratio of the V_T of the tissue and reference tissue:

$$DVr = \frac{V_T}{V_T'} = \frac{\frac{C_T(t)}{C_P(t)}}{\frac{C_T(t)'}{C_P(t)}} = \frac{C_T(t)}{C_T(t)'} = \frac{\frac{k1}{k2}}{\frac{k1'}{k2'}} = \frac{k1k2'}{k1'k2}$$

3.4 Validation methods

In the following, the validation methods used in the preclinical investigations of this thesis are described. They obtain long-established parameters, which are thus considered as reliable gold-standard for verification of PET. All have the disadvantage of requiring anaesthesia and mostly even euthanasia, which complicates or even prevents longitudinal experiments and results in high mouse numbers that are not consistent with the 3R-guidelines (reduce, refine, replace).

3.4.1 Histology and immunohistochemistry

Histology and immunohistochemistry are invasive procedures that provide cellular information of tissue samples. In preclinical experiments on mice, these are euthanized and their organs and tissues of interest are dissected, paraffin embedded and sectioned. The sections are stained, digitalized, and magnified for histological descriptive evaluations and semiquantitative scorings. These can be correlated with the signals and parameters obtained by PET.

Staining with HE is routinely used in research to get an overview before doing immunohistochemical stainings. It reveals characteristics of the cytoplasm, nucleus and extracellular matrix of a cell (57). In addition, other stainings can be performed, depending on the aspect to be examined. To visualize proliferative and apoptotic processes in cells, immunohistochemical staining with Ki-67 and cleaved Caspase3 is suitable (58).

With respect to proliferation measurement in a variety of human cancers, there is sufficient data that indicates a strong significant correlation between [^{18}F]FLT uptake and Ki-67 marker expression. Here, it is considered challenging that [^{18}F]FLT PET allows evaluation of a quite large tissue volume with information about regional heterogeneities, whereas Ki-67 immunohistochemistry examines a small tissue sample that often cannot account for such heterogeneities. One approach to compensate regional increases or decreases is to measure the average Ki-67 expression instead of the maximum Ki-67 expression.(8, 59)

Regarding the correlation of cleaved caspase3 immunohistochemistry and [^{18}F]ML-10 PET, there are only few published data. A preclinical study concerning neoadjuvant chemotherapy for triple-negative breast cancer showed an increased cleaved caspase3 level in the treated tumors compared to the tumor controls, but a decreased [^{18}F]ML-10 uptake. As a reason for this, the authors consider insufficient sensitivity of the radiotracer, problems in quantitative analysis or pH variations of the tumor microenvironment during the chemotherapy affecting [^{18}F]ML-10 uptake (60).

3.4.2 Biodistribution

Biodistribution is an invasive, ex vivo method to quantify and assess the in vivo behaviour and kinetics of radiotracers. In preclinical experiments on mice, the radiotracer is injected into their tail vein and they are euthanized at certain time points. Then the organs and tissues of interest are collected, weighed and measured for the amount of radioactivity, e.g. with the gammacounter Hidex AMG (Hidex, Mainz, Germany), which determines the amount of gamma-emitting nuclides in a sample using the scintillation principle. The resulting parameter is the percentage of injected dose per gram of tissue (%ID/g). This allows the pharmacokinetics and accumulation of the radiotracer to be evaluated and compared with the in vivo biodistribution obtained by PET.(61, 62)

It should be mentioned that although biodistribution is considered to be a gold-standard method, there are some sources of error in the technical performance, which can result in biased parameters. For example, it should be ensured that blood is removed from the collected organ, as this could contaminate the organ and thus increase the measured radiotracer amount. Tissues that do not belong to the organ, such as skin or fat, should also be completely removed. Following strict handling, the instruments would need to be changed after each collected organ or tissue to avoid contamination of the next one. Moreover, when using a gammacounter designed to measure low radioactivity, it should be ensured to keep dead times low. Thus, it can be concluded that biodistribution is sensitive to personnel or institutional variation due to different and not standardized techniques.(62)

A biodistribution study was planned and performed for publication I. We found strong variations in the measurement data with high standard deviations, which we assigned to the described potential error sources. As it was not possible to repeat the biodistribution study and improve the technical performance, the data were not included and discussed in the publication.

3.4.3 Blood analysis

A blood analysis includes examinations of the different blood cells and blood parameters and allows conclusion about blood formation, inflammation, infections or deficiencies. In preclinical experiments on mice, these are anesthetized and blood is collected from their facial vein. By means of a mouse blood analyser, e.g. scil VET abc (scil animal care company GmbH, Viernheim, Germany), and manual leukocyte differentiation, the number of WBC, RBC and PLT can be determined. The number of blood cells over time represents hematopoiesis and related proliferation and apoptosis and can be correlated with PET signals of the hematopoietic bone marrow. Whereas the blood parameters represent hematopoiesis globally, PET signals from the hematopoietic bone marrow can also provide regional information.

4. Conclusion

This thesis demonstrated that there are promising approaches for non-invasive, high-technology PET quantification that might serve as correlating surrogate for invasive, inconvenient methods.

The evaluation of the first approach of this thesis indicated that PET with the radiotracer [^{18}F]FLT has potential to visualize and detect proliferative processes due to irradiation induced cell damage. Especially with regard to proliferation in bone marrow, there was good agreement with the histological findings as well as the blood parameters. In contrast, PET with the radiotracer [^{18}F]ML-10 did not show such correlations and seemed to be not sensitive enough for imaging apoptotic processes due to irradiation induced cell damage.

The evaluation of the second approach of this theses showed promise that IDIF can facilitate the quantification of the diagnostic PET radiotracer [^{18}F]PI-2620 binding in brain, negating invasive arterial blood sampling. In order to differentiate patients with PSP and AD and healthy controls, the quantification parameter V_T was not sufficient enough for the examined cohort size, but V_T ratios or DV ratios using the inferior cerebellum as reference region were required. Additional studies need to focus on larger cohorts, radiometabolite analysis as well as plasma to whole blood ratios.

Overall, it was demonstrated that quantification approaches need to be evaluated and validated with gold-standard methods and that it can be challenging to identify the reason for non-correlating data. Especially the first approach of this thesis indicated that often many different aspects have to be included, such as the comparability of examination volumes, the sensitivity of radiotracers, the correct anatomical assignment of tissues and organs in the PET image and the precise technical performance with avoiding of personnel and institutional variations. The second approach of this thesis highlighted the importance of sufficiently large cohorts and, when scaling quantification parameters, the correct choice of reference tissues.

In conclusion, with the development of improved PET scanners and with the development of better performing quantification methods, in the future probably also with increasing use of artificial intelligence, invasive gold-standard methods may be gradually replaced by non-invasive PET.

5. Publications

5.1 List of publications

Original publications

This cumulative dissertation is in accordance with the graduation regulation for human biology in the medical faculty of the Ludwig-Maximilians-Universität München and based on the following two publications (publication I and II):

Meindl M, Bläske A, Steiger K, Lindner S, Lindheimer F, Lauber K, Brix N, von Ungern-Sternberg B, Oos R, Palumbo G, Böning, G, Schüle S, Majewski M, Port M, Ziegler S, Bartenstein P. Proliferation and Apoptosis after Whole-Body Irradiation: Longitudinal PET Study in a Mouse Model. European Journal of Nuclear Medicine and Molecular Imaging. 2024;51:395-404. https://doi.org/10.1007/s00259-023-06430-x

Meindl M, Zatcepin A, Gnörich J, Scheifele M, Zaganjori M, Groß M, Linder S, Lindner S, Schaefer R, Simmet M, Römer S, Katzdobler S, Levin J, Höglinger G, Bischof A, Barthel H, Sabri O, Bartenstein P, Saller T, Franzmeier N, Ziegler S, Brendel M. Assessment of [^{18}F]PI-2620 Tau-PET Quantification via Non-invasive Automatized Image Derived Input Function. European Journal of Nuclear Medicine and Molecular Imaging. 2024;51:3252-66. https://doi.org/10.1007/s00259-024-06741-7

Conference abstracts

The results of the investigations related to this doctoral thesis were additionally presented at national conferences:

Meindl M, Franzmeier N, Dilcher R, Wall S, Ferschmann C, Scheifele M, Beyer L, Eckenweber F, Bui N, Janowitz D, Rauchmann B, Katzdobler S, Perneczky R, Levin J, Bürger K, Barthel H, Sabri O, Bartenstein P, Ziegler S, Brendel M. Automatized image derived input function for quantification of 18-F-PI-2620 tau-PET imaging. Nuklearmedizin-NuclearMedicine. 2022;61(2):40.

Meindl M, Bläske A, Lindner S, Steiger K, Lauber K, Felbermeier M, Oos R, von Ungern-Sternberg B, Schüle S, Majewski M, Port M, Ziegler S, Bartenstein P. Änderung von Proliferation und Apoptose nach Strahlenexposition: Longitudinale PET-Studie im Mausmodell. Nuklearmedizin-NuclearMedicine. 2023;62(2):69.

Further publications

Within the scope of the investigations related to this doctoral thesis, contributions to the following publication were made:

Hong J, Brendel M, Erlandsson K, Sari H, Lu J, Clement C, Bui NV, **Meindl M**, Ziegler S, Barthel H, Sabri O, Choi H, Sznitman R, Rominger A, Shi K. Forecasting the Pharmacokinetics With Limited Early Frames in Dynamic Brain PET Imaging Using Neural Ordinary Differential Equation. IEEE Transactions on Radiation and Plasma Medical Sciences. 2023;7(6):607-17.

5.2 Contribution to publication I

My contribution to publication I, which was based on data collected in a preclinical setting, included in the first step an intensive examination of the already established study design. This involved the implementation of some changes, for example with regard to the time schedule or the subject numbers. In this context, I submitted an amendment request to the authority responsible for the approval of animal experiments, which was successfully accepted.

In the second step, I organized and performed all necessary experiments, starting with the procedure of ordering and receiving the animals as well as the mandatory daily health check of the animals and its documentation. I was responsible for the irradiation of the animals, for the performance of the positron emission tomography (PET) scans including the injection of the radiotracers and for the reconstruction of the PET images. I conducted invasive examinations such as biodistribution as well as organ removal and preservation for the histological and immunohistochemical investigations, which were subsequently performed at an external institute.

The third step involved the analysis and statistical testing of all data. Therefore I evaluated and quantified the PET images with the AMIDE software (open source) and correlated them with the results of the other examinations. In order to interpret the emerging trends and hypotheses correctly, a detailed literature review was necessary.

In the final step, I drafted an initial manuscript based on all findings, including self-designed figures and tables. This was further refined trough collaboration with the coauthors. As first and corresponding author, I was responsible for the submission and revision of the manuscript and the communication with the journals. Furthermore, I presented the results to the funder of the research project and at the conference of the German Society of Nuclear Medicine.

5.3 Contribution to publication II

My contribution to publication II was initially to support the conception and design of the studies, which were performed in a clinical setting. In this context, I established invasive blood sampling on study subjects for the determination of arterial input functions (AIF). This included the commissioning of the measuring device, the elaboration of the spatial arrangement of the entire measurement system, the testing of the measurement procedure and the performance of calibrations and error analyses. Apart from this, I developed a method using the PMOD software (PMOD Technologies, Zürich, Switzerland) to manually segment the carotid artery from a [^{18}F]PI-2620 PET image and determine image derived input functions (IDIF) for Logan plots. I was also involved in the development of an automated carotid artery segmentation method using Python.

After developing and establishing all methods, I applied them to a larger cohort consisting of controls and patients. With the determined input functions, I calculated various quantification parameters by again using the PMOD software. I performed a large evaluation of the input functions and quantification parameters and compared them by extensive statistical analysis.

I summarized the results and findings in a manuscript with several self-created figures and tables, which was iteratively extended and improved though collaboration with the coauthors. I was again responsible for the submission and revision process of the manuscript and the communication with the journals. I presented first results at the conference of the German Society of Nuclear Medicine.

6. References

1. Feng DD, Chen K, Wen L. Noninvasive input function acquisition and simultaneous estimations with physiological parameters for PET quantification: a brief review. IEEE Transactions on Radiation and Plasma Medical Sciences. 2020;4(6):676-83.

2. Somer E, Marsden P, Benatar N, Miquel M, O'Doherty M, Smith M. PET guided interventions and histological validation of PET. Nuclear Medicine Communications. 2004;25(4):420-1.

3. van der Weijden CW, Mossel P, Bartels AL, Dierckx RA, Luurtsema G, Lammertsma AA, et al. Non-invasive kinetic modelling approaches for quantitative analysis of brain PET studies. European Journal of Nuclear Medicine Molecular Imaging. 2023:1-15.

4. Cherry SR, Sorenson JA, Phelps ME. Physics in Nuclear Medicine: Saunders; 2012.

5. Bailey DL, Maisey MN, Townsend DW, Valk PE. Positron emission tomography: Springer; 2005.

6. Bailey DL, Humm J, Todd-Pokropek A, Van Aswegen A. Nuclear medicine physics: a handbook for teachers and students: International Atomic Energy Agency; 2014.

7. Lang F, Lang P. Basiswissen Physiologie: Springer-Verlag; 2007.

8. Salskov A, Tammisetti VS, Grierson J, Vesselle H. FLT: measuring tumor cell proliferation in vivo with positron emission tomography and 3′-deoxy-3′-[18F] fluorothymidine. Seminars in Nuclear Medicine. 2007;37(6):429-39.

9. Bollineni V, Kramer G, Jansma EP, Liu Y, Oyen W. A systematic review on [18F] FLT-PET uptake as a measure of treatment response in cancer patients. European Journal of Cancer. 2016;55:81-97.

10. Buck A, Herrmann K, Dechow T, Graf N, Schwaiger M, Wester H. Molekulare Bildgebung der Proliferation mit [18F] FLT-PET. Der Nuklearmediziner. 2009;32(02):154-63.

11. van Waarde A, Cobben DC, Suurmeijer AJ, Maas B, Vaalburg W, de Vries EF, et al. Selectivity of 18F-FLT and 18F-FDG for differentiating tumor from inflammation in a rodent model. Journal of Nuclear Medicine. 2004;45(4):695-700.

12. Strauss LG. Fluorine-18 deoxyglucose and false-positive results: a major problem in the diagnostics of oncological patients. European Journal of Nuclear Medicine. 1996;23:1409-15.

13. Metser U, Even-Sapir E. Increased 18F-fluorodeoxyglucose uptake in benign, nonphysiologic lesions found on whole-body positron emission tomography/computed tomography (PET/CT): accumulated data from four years of experience with PET/CT. Seminars in Nuclear Medicine. 2007;37(3):206-22.

14. Fried DV, Das SK, Marks LB. Imaging radiation-induced normal tissue injury to quantify regional dose response. Seminars in Radiation Oncology. 2017;27(4):325-31.

15. McGuire SM, Menda Y, Ponto LLB, Gross B, Buatti J, Bayouth JE. 3'-deoxy-3'-[18F] fluorothymidine PET quantification of bone marrow response to radiation dose. International Journal of Radiation Oncology* Biology* Physics. 2011;81(3):888-93.

16. Rendon DA, Kotedia K, Afshar SF, Punia JN, Sabek OM, Shirkey BA, et al. Mapping radiation injury and recovery in bone marrow using 18F-FLT PET/CT and USPIO MRI in a Rat Model. Journal of Nuclear Medicine. 2016;57(2):266-71.

17. Hartenbach M, Delker A, Hartenbach S, Schlichtiger J, Niedermoser S, Wängler C, et al. Dose-Dependent Uptake of 3′-deoxy-3′-[18 F] Fluorothymidine by the Bowel after Total-Body Irradiation. Molecular Imaging and Biology. 2014;16:846-53.

18. Agool A, Slart RH, Thorp KK, Glaudemans AW, Cobben DC, Been LB, et al. Effect of radiotherapy and chemotherapy on bone marrow activity: a 18F–FLT–PET study. Nuclear Medicine Communications. 2011;32(1):17-22.

19. Van de Wiele C, Ustmert S, De Spiegeleer B, De Jonghe P-J, Sathekge M, Alex M. Apoptosis imaging in oncology by means of positron emission tomography: a review. Internal Journal of Molecular Sciences. 2021;22(5):2753.

20. Kadirvel M, Fairclough M, Cawthorne C, Rowling EJ, Babur M, McMahon A, et al. Detection of apoptosis by PET/CT with the diethyl ester of [18F] ML-10 and fluorescence imaging with a dansyl analogue. Bioorganic & Medicinal Chemistry. 2014;22(1):341-9.

21. Reshef A, Shirvan A, Waterhouse RN, Grimberg H, Levin G, Cohen A, et al. Molecular imaging of neurovascular cell death in experimental cerebral stroke by PET. Journal of Nuclear Medicine. 2008;49(9):1520-8.

22. Jouberton E, Schmitt S, Maisonial-Besset A, Chautard E, Penault-Llorca F, Cachin F. Interest and Limits of [18F] ML-10 PET Imaging for Early Detection of Response to Conventional Chemotherapy. Frontiers in Oncology. 2021;11:5358.

23. Oborski MJ, Laymon CM, Lieberman FS, Drappatz J, Hamilton RL, Mountz JM. First use of 18F-labeled ML-10 PET to assess apoptosis change in a newly diagnosed glioblastoma multiforme patient before and early after therapy. Brain and Behaviour. 2014;4(2):312-5.

24. Sun L, Zhou K, Wang W, Zhang X, Ju Z, Qu B, et al. [18F] ML-10 imaging for assessment of apoptosis response of intracranial tumor early after radiosurgery by PET/CT. Contrast Media Molecular Imaging. 2018;2018.

25. Oborski MJ, Laymon CM, Qian Y, Lieberman FS, Nelson AD, Mountz JM. Challenges and approaches to quantitative therapy response assessment in glioblastoma multiforme using the novel apoptosis positron emission tomography tracer F-18 ML-10. Translational Oncology. 2014;7(1):111-9.

26. Allen AM, Ben-Ami M, Reshef A, Steinmetz A, Kundel Y, Inbar E, et al. Assessment of response of brain metastases to radiotherapy by PET imaging of apoptosis with 18 F-ML-10. Eurpoean Journal of Nuclear Medicine and Molecular Imaging. 2012;39:1400-8.

27. Gu B, Liu S, Sun Y, Zhang J, Zhang Y, Xu X, et al. Predictive Value of [18 F] ML-10 PET/CT in Early Response Evaluation of Combination Radiotherapy with Cetuximab on Nasopharyngeal Carcinoma. Molecular Imaging and Biology. 2019;21:538-48.

28. Fischer M, Olivier J, Lindner S, Zacherl MJ, Massberg S, Bartenstein P, et al. Detection of cardiac apoptosis by [18F] ML-10 in a mouse model of permanent LAD ligation. Molecular Imaging and Biology. 2022;24(4):666-74.

29. Fischer M, Zacherl MJ, Olivier J, Lindner S, Massberg S, Bartenstein P, et al. Detection of apoptosis by [18F] ML-10 after cardiac ischemia–reperfusion injury in mice. Annals of Nuclear Medicine. 2023;37(1):34-43.

30. Hyafil F, Tran-Dinh A, Burg S, Leygnac S, Louedec L, Milliner M, et al. Detection of apoptotic cells in a rabbit model with atherosclerosis-like lesions using the positron emission tomography radiotracer [18F] ML-10. Molecular Imaging 2015;14(8):433-42.

31. Song M, Beyer L, Kaiser L, Barthel H, van Eimeren T, Marek K, et al. Binding characteristics of [18F] PI-2620 distinguish the clinically predicted tau isoform in different tauopathies by PET. Journal of Cerebral Blood Flow Metabolism. 2021;41(11):2957-72.

32. Künze G, Kümpfel R, Rullmann M, Barthel H, Brendel M, Patt M, et al. Molecular Simulations Reveal Distinct Energetic and Kinetic Binding Properties of [18F] PI-2620 on Tau Filaments from 3R/4R and 4R Tauopathies. ACS Chemical Neuroscience. 2022;13(14):2222-34.

33. Kuang G, Murugan NA, Zhou Y, Nordberg A, Ågren H. Computational insight into the binding profile of the second-generation PET tracer PI2620 with tau fibrils. ACS Chemical Neuroscience. 2020;11(6):900-8.

34. Palleis C, Brendel M, Finze A, Weidinger E, Bötzel K, Danek A, et al. Cortical [18F] PI-2620 Binding Differentiates Corticobasal Syndrome Subtypes. Movement Disorders. 2021;36(9):2104-15.

35. Mueller A, Bullich S, Barret O, Madonia J, Berndt M, Papin C, et al. Tau PET imaging with 18F-PI-2620 in patients with Alzheimer disease and healthy controls: a first-in-humans study. Journal of Nuclear Medicine. 2020;61(6):911-9.

36. Brendel M, Barthel H, van Eimeren T, Marek K, Beyer L, Song M, et al. Assessment of 18F-PI-2620 as a biomarker in progressive supranuclear palsy. JAMA Neurology. 2020;77(11):1408-19.

37. Mormino EC, Toueg TN, Azevedo C, Castillo JB, Guo W, Nadiadwala A, et al. Tau PET imaging with 18 F-PI-2620 in aging and neurodegenerative diseases. European Journal of Nuclear Medicine and Molecular Imaging. 2021;48:2233-44.

38. Barret O, Seibyl J, Stephens A, Madonia J, Alagille D, Mueller A, et al. Initial clinical PET studies with the novel tau agent 18-F PI-2620 in Alzheimer's disease and controls. Soc Nuclear Med; 2017.

39. Oh M, Oh SJ, Lee SJ, Oh JS, Roh JH, Chung SJ, et al. Clinical evaluation of 18F-PI-2620 as a potent PET radiotracer imaging tau protein in Alzheimer disease and other neurodegenerative diseases compared with 18F-THK-5351. Clinical Nuclear Medicine. 2020;45(11):841-7.

40. Rullmann M, Brendel M, Schroeter ML, Saur D, Levin J, Perneczky RG, et al. Multicenter 18F-PI-2620 PET for in vivo Braak staging of tau pathology in Alzheimer's disease. Biomolecules. 2022;12(3):458.

41. Tezuka T, Takahata K, Seki M, Tabuchi H, Momota Y, Shiraiwa M, et al. Evaluation of [18F] PI-2620, a second-generation selective tau tracer, for assessing four-repeat tauopathies. Brain Communications. 2021;3(4):fcab190.

42. Thie JA. Understanding the standardized uptake value, its methods, and implications for usage. Journal of Nuclear Medicine. 2004;45(9):1431-4.

43. Kinahan PE, Fletcher JW. Positron emission tomography-computed tomography standardized uptake values in clinical practice and assessing response to therapy. Seminars in Ultrasound, CT and MRI. 2010;31(6):496-505.

44. Morris ED, Endres CJ, Schmidt KC, Christian BT, Muzic RF, Fisher RE. Kinetic modeling in positron emission tomography. Emission tomography: The fundamentals of PET and SPECT. 2004;46(1):499-540.

45. Innis RB, Cunningham VJ, Delforge J, Fujita M, Gjedde A, Gunn RN, et al. Consensus nomenclature for in vivo imaging of reversibly binding radioligands. Journal of Cerebral Blood Flow Metabolism. 2007;27(9):1533-9.

46. Su Y, Arbelaez AM, Benzinger TL, Snyder AZ, Vlassenko AG, Mintun MA, et al. Noninvasive estimation of the arterial input function in positron emission tomography imaging of cerebral blood flow. Journal of Cerebral Blood Flow Metabolism. 2013;33(1):115-21.

47. Munk OL, Keiding S, Bass L. A method to estimate dispersion in sampling catheters and to calculate dispersion-free blood time-activity curves. Medical Physics. 2008;35(8):3471-81.

48. Zanotti-Fregonara P, Chen K, Liow J-S, Fujita M, Innis RB. Image-derived input function for brain PET studies: many challenges and few opportunities. Journal of Cerebral Blood Flow Metabolism. 2011;31(10):1986-98.

49. Galovic M, Erlandsson K, Fryer TD, Hong YT, Manavaki R, Sari H, et al. Validation of a combined image derived input function and venous sampling approach for the quantification of [18F] GE-179 PET binding in the brain. NeuroImage. 2021;237:118194.

50. Sari H, Erlandsson K, Law I, Larsson HB, Ourselin S, Arridge S, et al. Estimation of an image derived input function with MR-defined carotid arteries in FDG-PET human studies using a novel partial volume correction method. Journal of Cerebral Blood Flow Metabolism. 2017;37(4):1398-409.

51. Bullich S, Barret O, Constantinescu C, Sandiego C, Mueller A, Berndt M, et al. Evaluation of dosimetry, quantitative methods, and test–retest variability of 18F-PI-2620 PET for the assessment of tau deposits in the human brain. Journal of Nuclear Medicine. 2020;61(6):920-7.

52. Logan J, Fowler JS, Volkow ND, Wolf AP, Dewey SL, Schlyer DJ, et al. Graphical analysis of reversible radioligand binding from time—activity measurements applied to [N-11C-methyl]-(−)-cocaine PET studies in human subjects. Journal of Cerebral Blood Flow Metabolism. 1990;10(5):740-7.

53. Logan J. A review of graphical methods for tracer studies and strategies to reduce bias. Nuclear medicine biology. 2003;30(8):833-44.

54. Kimura Y, Naganawa M, Shidahara M, Ikoma Y, Watabe H. PET kinetic analysis—Pitfalls and a solution for the Logan plot. Annals of Nuclear Medicine. 2007;21:1-8.

55. Lammertsma AA, Hume SP. Simplified reference tissue model for PET receptor studies. Neuroimage. 1996;4(3):153-8.

56. Wu Y, Carson RE. Noise reduction in the simplified reference tissue model for neuroreceptor functional imaging. Journal of Cerebral Blood Flow Metabolism. 2002;22(12):1440-52.

57. Fischer AH, Jacobson KA, Rose J, Zeller R. Hematoxylin and eosin staining of tissue and cell sections. Cold spring harbor protocols. 2008;2008(5).

58. Li Y, Cha S-B, Park Y, Gong B-H, Jeong I-Y, Kim H-S, et al. Evaluation of Caspase-3 and Ki-67 expression in squamous cell hyperplasia of the stomach induced by Platycodi radix water extract in Sprague–Dawley rats. Journal of toxicologic pathology. 2022;35(1):45-52.

59. Chalkidou A, Landau D, Odell E, Cornelius V, O'Doherty M, Marsden P. Correlation between Ki-67 immunohistochemistry and 18F-fluorothymidine uptake in patients with cancer: a systematic review and meta-analysis. European Journal of Cancer. 2012;48(18):3499-513.

60. Jouberton E, Schmitt S, Chautard E, Maisonial-Besset A, Roy M, Radosevic-Robin N, et al. [18 F] ML-10 PET imaging fails to assess early response to neoadjuvant chemotherapy in a preclinical model of triple negative breast cancer. EJNMMI research. 2020;10:1-14.

61. Lima BS, Videira MA. Toxicology and biodistribution: the clinical value of animal biodistribution studies. Molecular Therapy-Methods Clinical Development. 2018;8:183-97.

62. Chomet M, Schreurs M, Vos R, Verlaan M, Kooijman EJ, Poot AJ, et al. Performance of nanoScan PET/CT and PET/MR for quantitative imaging of 18F and 89Zr as compared with ex vivo biodistribution in tumor-bearing mice. EJNMMI research. 2021;11(1):57.

Danksagung

Nicht nur meine Promotion, sondern auch meine Zeit in „der NUK“ ist durch die Vollendung dieser Dissertation vorbei. Eine Zeit, die mich sehr geprägt hat, die mir die Welt des Arbeitslebens eröffnet hat und in der ich mich fachlich, wie auch persönlich weiterentwickeln durfte.

Um chronologisch zu beginnen, möchte ich mich zuallererst bei meiner Mama bedanken, ohne deren Einfall an einem sehr heißen Sommertag im August 2020 ich möglicherweise nie mit dem Fachgebiet der Nuklearmedizin und dem LMU Klinikum in Berührung gekommen wäre. Der Einfall beinhaltete, meinen Onkel Wolfgang zu kontaktieren - rückblickend war es perfektes Timing -, der wiederum den Kontakt zwischen Frau Ziegler und mir hergestellt hat. Danke Wolfgang!

Von da an durfte ich die Erfahrung einer menschlich wie auch fachlich wunderbaren Zusammenarbeit machen, die ich zu jedem Zeitpunkt sehr geschätzt habe und definitiv vermissen werde. Ich habe mich Woche für Woche auf unsere Freitags-Meetings gefreut, die hin und wieder auch mal etwas länger geraten sind und anregende Gespräche über unterschiedlichste Themen beinhalteten. Ich danke Ihnen für die viele Zeit, die Sie mir geschenkt haben, Frau Ziegler, für all die Dinge, die ich von Ihnen lernen durfte, für Ihren Rat bezüglich meiner beruflichen Zukunft und auch für Ihr stets vorhandenes Verständnis für Privates sowie das zuverlässige Schaffen der finanziellen Rahmenbedingungen.

All das und natürlich auch meine innerhalb kurzer Zeit entstandene Begeisterung für die Forschung und die Technologie der PET waren der Grund, warum ich im April 2021 plötzlich den Wunsch verspürt habe, entgegen der ursprünglichen Pläne und Vereinbarungen länger in der NUK zu bleiben und diese absolut nicht geplante Promotion durchzuführen. An dieser Stelle möchte ich mich bei meinem Papa bedanken, der mir durch seine Worte über seine eigenen Promotions-Erfahrungen den entscheidenden Impuls gegeben hat, diesem Wunsch nachzugehen.

Neben Frau Ziegler als meiner Doktormutter gilt mein großer Dank auch meinen anderen beiden Betreuern, Matthias und Kirsten, sowie unserem Chef Herrn Bartenstein. Durch dich, Matthias, habe ich einen sehr wertvollen Einblick in die Gehirn-Bildgebung erhalten und die Tiefen der PMOD-Welt kennengelernt. Dein biologischer Input bezüglich unserer nicht ganz leicht zu deutenden Signale des Gastrointestinaltrakts bzw. der mesenterialen Lymphknoten (wie auch immer ☺) war mir eine große Hilfe, Kirsten. Und woran ich mich immer gerne zurückerinnern werde, Herr Bartenstein, sind unsere [^{18}F]FLT- und [^{18}F]ML-10-Debatten, in die unter anderem auch die Erkenntnisse Ihrer wohlgemerkt 1985 abgeschlossenen Promotion eingeflossen sind.

Wer meine Zeit in der NUK natürlich auch maßgeblich geprägt und gestaltet hat, sind meine tollen, lieben Kollegen. Ich habe unsere vielen schönen Mittagessen ebenso geschätzt und genossen wie unsere gegenseitige, zuverlässige Hilfe und die gemeinsamen Kongresse in Leipzig. Besonders ans Herz gewachsen bist du mir, Astrid - für mich bist du mehr als eine Kollegin geworden. Du hast beruflich wie privat immer ein Ohr für mich gehabt und mir oftmals hilfreiche und wegweisende Ratschläge gegeben. Wofür ich dir auch sehr dankbar bin, ist, dass du mich in der MTRA-Schule integriert hast und ich dadurch einen Einblick in das Unterrichten erhalten konnte.

Zuallerletzt möchte ich mich bei Vali bedanken, den ich schon seit vielen Jahren kenne, dem ich als einer der ersten meiner Freunde von dieser Promotion erzählt habe und den ich mittlerweile meinen Lieblingsmenschen und Ehemann nennen darf. Auch wenn unsere Geschichte mein bis dahin ziemlich durchgeplantes Leben und meine Konzentration erst mal erheblich auf den Kopf

gestellt hat, ist es die schönste Geschichte, die mir passieren konnte. Dein liebevolles, tagtägliches Interesse für meine wohlgemerkt ganz andere Tätigkeit hat mir in der Schreibphase der beiden Paper und dieser Dissertation sehr viel Halt gegeben. An Tagen, die mal von Frustration und Ungeduld geprägt waren, hast du mich auf wunderbare Art und Weise aufgefangen und mir Mut zugesprochen. Und auch beim Brainstorming und der Entscheidungsfindung, wie es nach meiner Promotion für mich weitergehen soll, warst du mir eine große Hilfe. Danke!

Natürlich könnte ich noch viele weitere Personen aufzählen, die meine Promotion mitbegleitet haben, sei es Familie oder Freunde. Sehr bedauere ich, dass meine ebenfalls promovierte „Penzing-Oma“ die Veröffentlichung meiner beiden Paper und die Vollendung dieser Dissertation nicht mehr miterleben kann - zum Glück kann das aber meine andere liebe und stolze Oma. Um den Rahmen dieser Danksagung nicht zu sprengen, sage ich abschließend ein großes Danke an alle Wegbegleiter, die ich hier nicht namentlich erwähnt habe!